

Supplementary Materials for **Precision Spectroscopy of Polarized Molecules in an Ion Trap**

H. Loh,* K. C. Cossel, M. C. Grau, K.-K. Ni,
E. R. Meyer, J. L. Bohn, J. Ye,* E. A. Cornell*

*Corresponding author. E-mail: loh@jila.colorado.edu (H.L.);
ye@jila.colorado.edu (J.Y.); cornell@jila.colorado.edu (E.A.C.)

Published 6 December 2013, *Science* **342**, 1220 (2013)
DOI: 10.1126/science.1243683

This PDF file includes:

Materials and Methods
Supplementary Text
Figs. S1 and S2
References

Materials and Methods

The experiment sequence starts with the creation of neutral HfF molecules from ablating a Hf rod in the presence of a gas comprising 1% SF₆ and 99% Ar. The gas is released into the vacuum chamber through the opening of a pulsed valve (800 μm orifice, 830 kPa backing pressure) for 180 μs. The neutral HfF molecules are cooled by supersonic expansion to a translational and rotational temperature of ~10 K. To create HfF⁺, we cross two pulsed lasers (309 nm, 368 nm) with the supersonic beam downstream of the ablation to excite ground state neutral HfF molecules to a Rydberg state with an excited ion core. The Rydberg molecules can then autoionize to form ¹⁸⁰Hf¹⁹F⁺ ions, 35% of which are in the ¹Σ₀⁺ ($v'' = 0, J'' = 0$) ground rovibronic state (32).

The ionization process takes place inside the center of the ion trap, so that upon ionization, we can immediately stop the ions with a pulsed stopping field and then trap them with the linear quadrupole Paul trap. The rotating bias field is ramped on by applying an additional set of sinusoidal voltages to the radial-confinement electrodes on top of the trapping radiofrequency (RF) and direct current (DC) voltages. Under the influence of the rotating bias field and trapping fields, the ions undergo a combination of secular harmonic motion at $\omega_{\text{sec}}/(2\pi) = 5$ kHz, trap-RF-induced micromotion at $\omega_{\text{RF}}/(2\pi) = 50$ kHz and rotating-bias-field-induced circular micromotion at $\omega_{\text{rot}}/(2\pi) = 253$ kHz in the radial plane. (In the axial direction, the ions experience only secular harmonic motion at $\omega_z/(2\pi) = 0.8\text{-}3.6$ kHz.)

In the presence of the rotating bias field, we populate ions in a desired Stark level-pair of the ³Δ₁ ($v = 0, J = 1, F = 3/2$) state using two Raman transfer lasers. The first transfer laser at 900 nm drives the ³Π₀₊ ($v' = 1, J' = 1$) ← ¹Σ₀⁺ ($v'' = 0, J'' = 0$) transition while the second transfer laser at 986 nm drives the ³Π₀₊ ($v' = 1, J' = 1$) → ³Δ₁ ($v = 0, J = 1, F = 3/2$) transition (33). Both lasers are detuned by 160 MHz from their respective one-photon resonances to avoid populating the

$^3\Pi_{0+}$ excited state. Light from both lasers is simultaneously directed onto the ions through the top electrode of the ion trap for 1.2 ms, during which the trapped ions' axial motion Doppler-shift the transfer laser frequencies to sweep through the two-photon detuning. The desired Stark level-pair is populated when the two-photon resonance condition is fulfilled.

To deplete ions from the $|m_F = -3/2\rangle$ sublevel within a Stark level-pair, we direct a σ^+ -polarized depletion laser, tuned to resonance with the $^3\Pi_{0+} (\nu' = 1, J' = 1) \rightarrow ^3\Delta_1 (\nu = 0, J = 1, F = 3/2)$ transition, between two radially-confining trap electrodes onto the ions. The depletion laser is stroboscopically turned on, with a duty cycle of 20%, whenever the rotating quantization axis lies roughly parallel to the direction of laser propagation. 250 rotation cycles (about 1 ms) are needed to fully deplete the ions from one of the two m_F sublevels. In the absence of a rotating magnetic field, the depletion laser acts as a $\pi/2$ pulse because the remaining ions are left in a single $|m_F\rangle$ sublevel, which is an equal superposition of the eigenstates $|\pm\rangle_{B_{rot}=0}$.

For experiments where a rotating magnetic field is needed, the static magnetic field gradient is applied prior to ionization by running current through a pair of anti-Helmholtz coils positioned just outside the ion trap. The radial magnetic field gradient can be increased up to 1.65 G/cm, which corresponds to an effective rotating magnetic field up to 0.037 G for a circular micromotion radius of 0.22 mm obtained with a rotating electric field of 11.6 V/cm. Reversing the sign of the rotating magnetic field from positive to negative is accomplished by changing the direction of applied current, such that the magnetic field gradient points radially outwards instead of inwards. The static magnetic field component $\mathbf{B}_{\text{static}}$ acting on our rotating eigenstates generates nothing but a negligible ($< 10^{-3}$) phase modulation over a period of rotation. A displacement of the null of the static magnetic-field quadrupole relative to the trap center along the radial or axial directions therefore also exerts a negligible effect because it merely affects $\mathbf{B}_{\text{static}}$ and not \mathbf{B}_{rot} , and because the quantization axis is nearly entirely defined by electric and not magnetic fields. Ref.

(2) offers a more in-depth analysis of the negligible effects of static magnetic-field gradient misalignments on precision spectroscopy.

Finally, to detect the ions in a particular m_F sublevel after the Ramsey sequence, we use the depletion strobe-sequence to optically pump away ion population in the undesired m_F sublevel without depopulating the desired sublevel, before photodissociating the ions remaining in the $J = 1$ state with 286 nm and 266 nm pulsed lasers. The dissociated ions are counted on a microchannel plate as Hf^+ atomic ions, mass-resolved from HfF^+ in time-of-flight. The 286 nm photon drives a bound-bound transition within the HfF^+ molecule and provides rotational-state selectivity to the dissociation. A manuscript on the photodissociation process is being prepared.

Supplementary Text

Rotating-frame Hamiltonian

Within either the uppermost or lowermost Stark level-pair, the two sublevels $\{|m_F = 3/2\rangle, |m_F = -3/2\rangle\}$ could be coherently coupled to each other via a three-photon transition. Alternative to using three radiofrequency photons, we can take advantage of the coupling (via third-order perturbative process) already provided by the rotation of the electric field.

The rotating-frame Hamiltonian is expressed in the $\{|m_F = +3/2\rangle, |m_F = -3/2\rangle\}$ basis as follows (2):

$$H = \begin{pmatrix} -\frac{3}{2}g_F\mu_B B_{\text{rot}} & \frac{\Delta}{2} \\ \frac{\Delta}{2} & \frac{3}{2}g_F\mu_B B_{\text{rot}} \end{pmatrix}, \quad (\text{S1})$$

where g_F is the magnetic g-factor for the $F = 3/2$ state, μ_B is the Bohr magneton, B_{rot} is the rotating magnetic field and Δ is the splitting between the energy eigenstates at $B_{\text{rot}} = 0$. The coupling energy Δ , which arises from the rotation of the quantization axis, is very similar for both the uppermost and lowermost Stark level-pairs $\Delta^{u/l}$. For a three-photon transition necessary to

connect the $m_F = \pm 3/2$ states, the average of Δ for the two Stark pairs is proportional to the ratio of the rotation frequency ω_{rot} to the Stark energy $d_{\text{mf}}E_{\text{rot}}$, raised to the power of three:

$$\Delta = \frac{1}{2}(\Delta^l + \Delta^u) = 27\hbar\omega_{\text{ef}} \left(\frac{\hbar\omega_{\text{rot}}}{d_{\text{mf}}E_{\text{rot}}} \right)^3. \quad (\text{S2})$$

Δ is also proportional to the energy splitting between the parity eigenstates at zero electric field ω_{ef} , which sets the scale of the coupling between states with opposite sign Ω (where Ω is the projection of total angular momentum onto the molecular axis).

There is a slight frequency difference between Δ for the two Stark pairs, which comes from interactions with the nearest $F = 1/2$ hyperfine level, detuned from the $F = 3/2$ manifold by E_{HF} . Specifically, the upper Stark pair is more repelled from the $F = 1/2$ levels than the lower Stark pair. Perturbation theory on the Hilbert space of twelve $|F, m_F, \Omega\rangle$ sublevels in the ${}^3\Delta_1$ ($v = 0, J = 1$) rotational state yields the following expression for $\delta\Delta$:

$$\delta\Delta = \frac{1}{2}(\Delta^l - \Delta^u) = \frac{81}{8}\hbar\omega_{\text{ef}} \left(\frac{\hbar\omega_{\text{rot}}}{d_{\text{mf}}E_{\text{rot}}} \right)^3 \left(\frac{d_{\text{mf}}E_{\text{rot}}}{E_{\text{HF}}} \right). \quad (\text{S3})$$

We note that the numerical coefficients in Eqs. (S2)-(S3) were calculated numerically for Ref. (2), but there was an error in transcribing the results to that manuscript. The expressions presented here are analytical results from perturbation theory and are consistent with revised numerical calculations.

Figure S1 shows an experimental verification of the third-order dependence of Δ on $1/E_{\text{rot}}$, measured by repeating the Ramsey spectroscopy technique for different values of E_{rot} . The lines come from a simultaneous fit to Δ^u and Δ^l using Eqs. (S2)-(S3). The sole adjustable parameter, $\omega_{\text{ef}}/(2\pi)$, is determined to be 830(50) kHz. $\omega_{\text{ef}}/(2\pi)$ was independently determined in Ref. (33) to be 740(20) kHz, and the two measurements agree to within two standard deviations.

We take advantage of the strong dependence of the avoided-crossing splitting and its eigenstates on E_{rot} (Fig. S2) to execute $\pi/2$ pulses at high magnetic fields. For a given finite

magnetic field, we can ramp E_{rot} to an appropriate lower value and back in order to project the initial $|m_F\rangle$ state onto an equal superposition of the energy eigenstates $|\pm\rangle$.

The full avoided-crossing energy measured as a function of B_{rot} for either the upper or lower Stark pair, as shown in Fig. 3, is fit to the following function:

$$\frac{\omega^{u/l}}{2\pi} = 2 \sqrt{\left(\frac{\Delta^{u/l}}{2h}\right)^2 + \left(\frac{3}{2} \mu_B g_F^{u/l} (B_{\text{rot}} - B_{\text{offset}}^{u/l})\right)^2}, \quad (\text{S4})$$

where $B_{\text{offset}}^{u/l}$ is a magnetic field offset that shifts the avoided crossing away from zero along the horizontal axis. The fit parameters yield $\Delta^u/h = 25(1)$ Hz and $\Delta^l/h = 36(1)$ Hz, which are in good agreement with that expected from Eqs. (S2)-(S3). The magnetic field offsets fit to $B_{\text{offset}}^u = 0.15(11)$ mG and $B_{\text{offset}}^l = 0.02(9)$ mG. The average of both offsets is roughly that expected from driving currents up and down the radial confinement electrodes to provide the rotating bias field. The difference between the two offsets, which is proportional to the eEDM signal, is consistent with zero. Combined with the theoretical value for the effective electric field on the electron $E_{\text{eff}} = 24$ GV/cm (19, 34), the difference in B_{offset} yields a preliminary eEDM limit of 1.5×10^{-25} e·cm.

The eEDM statistical uncertainty can potentially average to 1×10^{-28} e·cm in 12 hours assuming 4 detected ions making the Ramsey transition, a 150 ms coherence time, and a 4 Hz repetition rate for the experimental cycle. The systematic uncertainties have been estimated in Ref. (2) to be on the order of 10^{-29} e·cm.

Sign of the magnetic g-factor

When the rotating quantization axis is tilted away from the plane of rotation by a small angle α , such that one rotation traces out a cone with opening half-angle $\pi/2 - \alpha$ and solid angle Ω_{SA} , the ions in a given m_F level accumulate a Berry phase shift (22)

$$\phi_{\text{Berry}} = -m_F \Omega_{\text{SA}} = -m_F 2\pi(1 - \sin(\alpha)). \quad (\text{S5})$$

The resulting phase shift on the spin state $|m_F\rangle$, over one rotation period $\tau = (2\pi)/\omega_{\text{rot}}$, is

correspondingly $e^{-i\omega_m\tau} e^{i\phi_{\text{Berry}}} = e^{-i(\omega_m - \frac{\phi_{\text{Berry}}}{\tau})\tau}$, where ω_m is the Zeeman frequency. The Berry phase, modulo an integer multiple of π , translates to a frequency shift of (2)

$$\omega_{\text{Berry}} = -\frac{\phi_{\text{Berry}}}{\tau} = m_F \frac{\omega_{\text{rot}}}{2\pi} (2\pi)(-\sin(\alpha)) \approx -m_F \omega_{\text{rot}} \alpha. \quad (\text{S6})$$

In the case of the quantization axis rotating about a small tipping angle ($\pi/2 - \alpha \ll 1$), one can describe the Berry-phase frequency shift instead as a sort of low-frequency AC Stark perturbation (35, 36). For the maximal tipping angle of $\pi/2$, however, that perturbative approach does not yield useful intuition. To verify the simple Berry phase result (S6) above, one may instead laboriously rediagonalize the problem in a rotating frame (23).

To impart a Berry phase, we deliberately kick the ions above or below the plane of rotation. The maximum tilt angle of the quantization axis is then given by $\alpha = E_{z,\text{max}}/E_{\text{rot}}$, where $E_{z,\text{max}}$ is the maximum axial trapping field experienced by the ions as they oscillate away from the plane of rotation (i.e. $E_{z,\text{max}} < 0$ for an upward kick). The diagonal terms of the Hamiltonian in Eq. (S1) in turn become $\mp m_F g_F \mu_B B_{\text{rot}} + \omega_{\text{Berry}} \sin(\omega_z t)$, where $\sin(\omega_z t) > 0$ in half an axial trap cycle.

Relating the energies of the sublevels back to experimental parameters, we obtain the following dependence for the sign of ω_{Berry} :

$$\text{sign}(\omega_{\text{Berry}}) = + \text{sign}(m_F) \text{sign}(\omega_{\text{rot}}) \text{sign}(\text{kick}), \quad (\text{S7})$$

where ω_{rot} is positive (negative) if the quantization axis rotates counter-clockwise (clockwise), and $\text{sign}(\text{kick})$ is positive (negative) if the ions are kicked upwards (downwards).

Our convention for the sign of the magnetic g-factor is defined in Eq. (S1). Therefore, the sign of the Zeeman energy is

$$\text{sign}(\text{Zeeman energy}) = - \text{sign}(m_F) \text{sign}(g_F) \text{sign}(|\mu_B|) \text{sign}(B'), \quad (\text{S8})$$

where B' parameterizes the static magnetic field as $B = B' z\hat{z} - \frac{B'}{2} \rho\hat{\rho}$. Since $\mathbf{B}_{\text{rot}} = \mathbf{r}_{\text{rot}} \partial B_{\text{rot}} / \partial \rho$

and $\mathbf{r}_{\text{rot}} \propto -\mathbf{E}_{\text{rot}}$ for circular motion, $\text{sign}(B') = \text{sign}(B_{\text{rot}})$.

It then follows from Eqs. (S7) and (S8) that

$$\text{sign}(g_F) = -\text{sign}(B') \text{ sign}(\omega_{\text{rot}}) \text{ sign(fringe frequency)} \text{ sign(kick)}, \quad (\text{S9})$$

where $\text{sign(fringe frequency)}$ is positive if the fringe frequency increases. Applying Eq. (S9) to the data presented in Fig. 4, taken with $B' > 0$ and $\omega_{\text{rot}} > 0$, g_F is determined to be positive.

Having understood the effect of Berry phase, we note that during an actual precision measurement, care must be taken to collect data asynchronously with any unintended initial axial slosh of the ions' center of mass, so as to minimize systematic errors associated with Berry phase. This should not pose a major technical challenge.

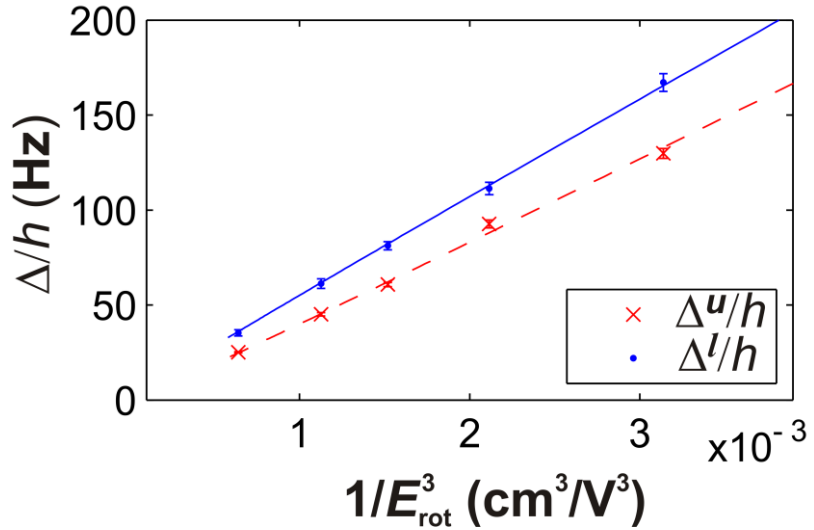


Fig. S1. Measurement of avoided-crossing splitting at zero rotating magnetic field.

Ramsey fringe frequency (Δ/h) measured as a function of the magnitude of the rotating-bias-field E_{rot} (red crosses for the upper Stark pair and blue dots for the lower Stark pair). The lines are a single-adjustable-parameter fit to the data using theory describing the rotating-frame Hamiltonian (2).

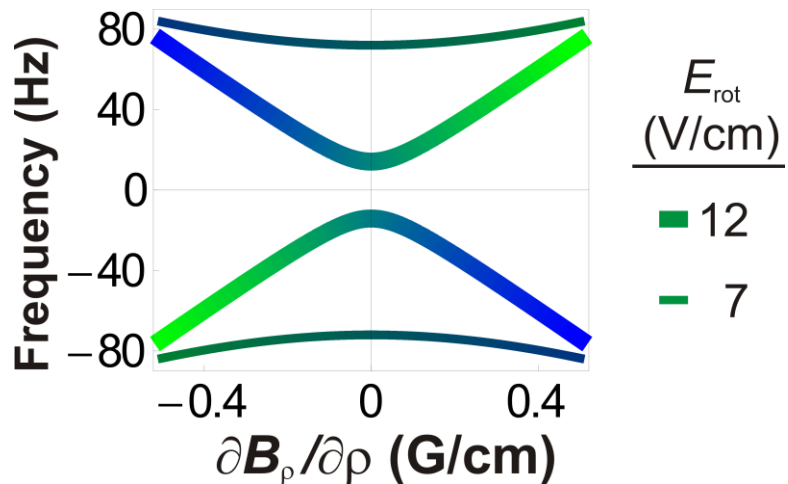


Fig. S2. Avoided-crossing splitting as a function of applied magnetic-field gradient.

Theory curves describing the avoided crossing, plotted with two different line thicknesses for the two values of E_{rot} . The eigenstates are depicted as superpositions of the colors blue (for $|m_F = 3/2\rangle$) and green (for $|m_F = -3/2\rangle$). For a given magnetic-field gradient (e.g. 0.4 G/cm), the eigenstates can change from being almost pure $|m_F\rangle$ states at $E_{\text{rot}} = 12$ V/cm to near-equal superpositions of the two $|m_F\rangle$ states at $E_{\text{rot}} = 7$ V/cm.

References

1. L. D. Carr, D. DeMille, R. V. Krems, J. Ye, Cold and ultracold molecules: Science, technology and applications. *New J. Phys.* **11**, 055049 (2009). [doi:10.1088/1367-2630/11/5/055049](https://doi.org/10.1088/1367-2630/11/5/055049)
2. A. E. Leanhardt, J. L. Bohn, H. Loh, P. Maletinsky, E. R. Meyer, L. C. Sinclair, R. P. Stutz, E. A. Cornell, High-resolution spectroscopy on trapped molecular ions in rotating electric fields: a new approach for measuring the electron electric dipole moment. *J. Mol. Spectrosc.* **270**, 1–25 (2011). [doi:10.1016/j.jms.2011.06.007](https://doi.org/10.1016/j.jms.2011.06.007)
3. S. Willitsch, M. T. Bell, A. D. Gingell, T. P. Softley, Chemical applications of laser- and sympathetically-cooled ions in ion traps. *Phys. Chem. Chem. Phys.* **10**, 7200–7210 (2008). [doi:10.1039/b813408c](https://doi.org/10.1039/b813408c) [Medline](#)
4. P. F. Staanum, K. Hojbjerre, P. S. Skyt, A. K. Hansen, M. Drewsen, Rotational laser cooling of vibrationally and translationally cold molecular ions. *Nat. Phys.* **6**, 271–274 (2010). [doi:10.1038/nphys1604](https://doi.org/10.1038/nphys1604)
5. J. H. V. Nguyen, C. R. Viteri, E. G. Hohenstein, C. D. Sherrill, K. R. Brown, B. Odom, Challenges of laser-cooling molecular ions. *New J. Phys.* **13**, 063023 (2011). [doi:10.1088/1367-2630/13/6/063023](https://doi.org/10.1088/1367-2630/13/6/063023)
6. U. Bressel, A. Borodin, J. Shen, M. Hansen, I. Ernsting, S. Schiller, Manipulation of individual hyperfine states in cold trapped molecular ions and application to HD⁺ frequency metrology. *Phys. Rev. Lett.* **108**, 183003 (2012). [doi:10.1103/PhysRevLett.108.183003](https://doi.org/10.1103/PhysRevLett.108.183003) [Medline](#)
7. S. Ding, D. Matsukevich, Quantum logic for the control and manipulation of molecular ions using a frequency comb. *New J. Phys.* **14**, 023028 (2012). [doi:10.1088/1367-2630/14/2/023028](https://doi.org/10.1088/1367-2630/14/2/023028)
8. J. E. Goeders, C. R. Clark, G. Vittorini, K. Wright, C. R. Viteri, K. R. Brown, Identifying single molecular ions by resolved sideband measurements. *J. Phys. Chem. A* **117**, 9725–9731 (2013). [doi:10.1021/jp312368a](https://doi.org/10.1021/jp312368a) [Medline](#)
9. W. G. Rellergert, S. T. Sullivan, S. J. Schowalter, S. Kotochigova, K. Chen, E. R. Hudson, Evidence for sympathetic vibrational cooling of translationally cold molecules. *Nature* **495**, 490–494 (2013). [doi:10.1038/nature11937](https://doi.org/10.1038/nature11937) [Medline](#)
10. J. K. Thompson, S. Rainville, D. E. Pritchard, Cyclotron frequency shifts arising from polarization forces. *Nature* **430**, 58–61 (2004). [doi:10.1038/nature02682](https://doi.org/10.1038/nature02682) [Medline](#)
11. D. I. Schuster, L. S. Bishop, I. L. Chuang, D. DeMille, R. J. Schoelkopf, Cavity QED in a molecular ion trap. *Phys. Rev. A* **83**, 012311 (2011). [doi:10.1103/PhysRevA.83.012311](https://doi.org/10.1103/PhysRevA.83.012311)
12. J. J. Hudson, D. M. Kara, I. J. Smallman, B. E. Sauer, M. R. Tarbutt, E. A. Hinds, Improved measurement of the shape of the electron. *Nature* **473**, 493–496 (2011). [doi:10.1038/nature10104](https://doi.org/10.1038/nature10104) [Medline](#)
13. I. B. Khriplovich, S. K. Lamoreaux, *CP Violation Without Strangeness: Electric Dipole Moments of Particles, Atoms and Molecules* (Springer, Berlin, 1997).

14. E. D. Commins, in *Advances in Atomic, Molecular and Optical Physics*, vol. 40, B. Bederson, H. Walther, Eds. (Academic Press, 1999), pp. 1–55.
15. D. DeMille, F. Bay, S. Bickman, D. Kawall, D. Krause, S. Maxwell, L. Hunter, Investigation of PbO as a system for measuring the electric dipole moment of the electron. *Phys. Rev. A* **61**, 052507 (2000). [doi:10.1103/PhysRevA.61.052507](https://doi.org/10.1103/PhysRevA.61.052507)
16. S. Eckel, P. Hamilton, E. Kirilov, H. W. Smith, D. DeMille, Search for the electron electric dipole moment using Ω -doublet levels in PbO. *Phys. Rev. A* **87**, 052130 (2013). [doi:10.1103/PhysRevA.87.052130](https://doi.org/10.1103/PhysRevA.87.052130)
17. A. C. Vutha, W. C. Campbell, Y. V. Gurevich, N. R. Hutzler, M. Parsons, D. Patterson, E. Petrik, B. Spaun, J. M. Doyle, G. Gabrielse, D. DeMille, Search for the electric dipole moment of the electron with thorium monoxide. *J. Phys. B* **43**, 074007 (2010). [doi:10.1088/0953-4075/43/7/074007](https://doi.org/10.1088/0953-4075/43/7/074007)
18. E. R. Meyer, J. L. Bohn, M. P. Deskevich, Candidate molecular ions for an electron electric dipole moment experiment. *Phys. Rev. A* **73**, 062108 (2006). [doi:10.1103/PhysRevA.73.062108](https://doi.org/10.1103/PhysRevA.73.062108)
19. A. N. Petrov, N. S. Mosyagin, T. A. Isaev, A. V. Titov, Theoretical study of HfF⁺ in search of the electron electric dipole moment. *Phys. Rev. A* **76**, 030501 (2007). [doi:10.1103/PhysRevA.76.030501](https://doi.org/10.1103/PhysRevA.76.030501)
20. E. R. Meyer, J. L. Bohn, Prospects for an electron electric-dipole moment search in metastable ThO and ThF⁺. *Phys. Rev. A* **78**, 010502 (2008). [doi:10.1103/PhysRevA.78.010502](https://doi.org/10.1103/PhysRevA.78.010502)
21. Supplementary materials are available on *Science Online*.
22. M. V. Berry, Quantal phase factors accompanying adiabatic changes. *Proc. R. Soc. Lond. A Math. Phys. Sci.* **392**, 45–57 (1984). [doi:10.1098/rspa.1984.0023](https://doi.org/10.1098/rspa.1984.0023)
23. E. R. Meyer, A. E. Leanhardt, E. A. Cornell, J. L. Bohn, Berry-like phases in structured atoms and molecules. *Phys. Rev. A* **80**, 062110 (2009). [doi:10.1103/PhysRevA.80.062110](https://doi.org/10.1103/PhysRevA.80.062110)
24. J. M. Pendlebury, W. Heil, Y. Sobolev, P. Harris, J. Richardson, R. Baskin, D. Doyle, P. Geltenbort, K. Green, M. van der Grinten, P. Iaydjiev, S. Ivanov, D. May, K. Smith, Geometric-phase-induced false electric dipole moment signals for particles in traps. *Phys. Rev. A* **70**, 032102 (2004). [doi:10.1103/PhysRevA.70.032102](https://doi.org/10.1103/PhysRevA.70.032102)
25. M. Rupasinghe, N. E. Shafer-Ray, Effect of the geometric phase on the possible measurement of the electron's electric dipole moment using molecules confined by a Stark gravitational trap. *Phys. Rev. A* **78**, 033427 (2008). [doi:10.1103/PhysRevA.78.033427](https://doi.org/10.1103/PhysRevA.78.033427)
26. D. Porras, J. I. Cirac, Effective quantum spin systems with trapped ions. *Phys. Rev. Lett.* **92**, 207901 (2004). [doi:10.1103/PhysRevLett.92.207901](https://doi.org/10.1103/PhysRevLett.92.207901) [Medline](#)
27. K. Kim, M. S. Chang, R. Islam, S. Korenblit, L. M. Duan, C. Monroe, Entanglement and tunable spin-spin couplings between trapped ions using multiple transverse modes. *Phys. Rev. Lett.* **103**, 120502 (2009). [doi:10.1103/PhysRevLett.103.120502](https://doi.org/10.1103/PhysRevLett.103.120502) [Medline](#)

28. J. W. Britton, B. C. Sawyer, A. C. Keith, C. C. Wang, J. K. Freericks, H. Uys, M. J. Biercuk, J. J. Bollinger, Engineered two-dimensional Ising interactions in a trapped-ion quantum simulator with hundreds of spins. *Nature* **484**, 489–492 (2012). [doi:10.1038/nature10981](https://doi.org/10.1038/nature10981) [Medline](#)
29. V. V. Flambaum, M. G. Kozlov, Enhanced sensitivity to the time variation of the fine-structure constant and m_p/m_e in diatomic molecules. *Phys. Rev. Lett.* **99**, 150801 (2007). [doi:10.1103/PhysRevLett.99.150801](https://doi.org/10.1103/PhysRevLett.99.150801) [Medline](#)
30. H. Müller, S. Herrmann, A. Saenz, A. Peters, C. Lammerzahl, Tests of Lorentz invariance using hydrogen molecules. *Phys. Rev. D Part. Fields Gravit. Cosmol.* **70**, 076004 (2004). [doi:10.1103/PhysRevD.70.076004](https://doi.org/10.1103/PhysRevD.70.076004)
31. J. Baron, W. C. Campbell, D. DeMille, J. M. Doyle, G. Gabrielse, Y. V. Gurevich, P. W. Hess, N. R. Hutzler, E. Kirilov, I. Kozyryev, B. R. O'Leary, C. D. Panda, M. F. Parsons, E. S. Petrik, B. Spaun, A. C. Vutha, A. D. West, ACME Collaboration, Order of magnitude smaller limit on the electric dipole moment of the electron (2013); arXiv:1310.7534.
- 32.. H. Loh, J. Wang, M. Grau, T. S. Yahn, R. W. Field, C. H. Greene, E. A. Cornell, Laser-induced fluorescence studies of HfF^+ produced by autoionization. *J. Chem. Phys.* **135**, 154308 (2011). [doi:10.1063/1.3652333](https://doi.org/10.1063/1.3652333) [Medline](#)
33. K. Cossel, D. N. Gresh, L. C. Sinclair, T. Coffey, L. V. Skripnikov, A. N. Petrov, N. S. Mosyagin, A. V. Titov, R. W. Field, E. R. Meyer, E. A. Cornell, J. Ye, Broadband velocity modulation spectroscopy of HfF^+ : Towards a measurement of the electron electric dipole moment. *Chem. Phys. Lett.* **546**, 1–11 (2012). [doi:10.1016/j.cplett.2012.06.037](https://doi.org/10.1016/j.cplett.2012.06.037)
34. T. Fleig, M. K. Nayak, Electron electric-dipole-moment interaction constant for HfF^+ from relativistic correlated all-electron theory. *Phys. Rev. A* **88**, 032514 (2013). [doi:10.1103/PhysRevA.88.032514](https://doi.org/10.1103/PhysRevA.88.032514)
35. N. F. Ramsey, Resonance transitions induced by perturbations at two or more different frequencies. *Phys. Rev.* **100**, 1191–1194 (1955). [doi:10.1103/PhysRev.100.1191](https://doi.org/10.1103/PhysRev.100.1191)
36. N. F. Ramsey, A molecular beam resonance method with separated oscillating fields. *Phys. Rev.* **78**, 695–699 (1950). [doi:10.1103/PhysRev.78.695](https://doi.org/10.1103/PhysRev.78.695)